DTU

DTU Library

Unidirectional-propagating surface magnetoplasmon based on remanence and its application for subwavelength isolators

You, Yun; Xiao, Sanshui ; Wu, Chiaho; Zhang, Hang; Deng, Xiaohua; Shen, Linfang

Unidirectional-propagating surface magnetoplasmon based on remanence and its application for subwavelength isolators

Yun You,[1,2] Sanshui Xiao,[3,5] Chiaho Wu,[4] Hang Zhang,[4] Xiaohua Deng,[2] and Linfang Shen[4,*]

[1]*College of Material Science and Engineering, Nanchang University, Nanchang, 330031, China*
[2]*Institute of Space Science and Technology, Nanchang University, Nanchang, 330031, China*
[3]*Department of Photonics Engineering, Technical University of Denmark, DK-2800 Kgs. Lyngby, Denmark*
[4]*Department of Applied Physics, Zhejiang University of Technology, Hangzhou 310023, China*
[5]*saxi@fotonik.dtu.dk*
[*]*lfshen@zjut.edu.cn*

Abstract: Ferrimagnetic material with remanence holds the potential to realize unidirectional propagation of the electromagnetic field by taking advantage of magnetoplasmon in the sub-wavelength regime. Here, we theoretically investigate magnetoplasmons in a layered structure consisting of a dielectric sandwiched by two magnetic materials with anti-parallel remanent magnetization directions, which shows a complete unidirectional propagating region for both even and odd symmetry modes when the thickness of the dielectric is smaller than a certain value. Additionally, the even symmetry mode supported by such a one-way waveguide can be effectively, with low insertion loss, excited by the fundamental transverse-electric mode of a traditional metal slab waveguide. Relying on low insertion loss and a one-way propagation feature, we propose a broadband and subwavelength isolator working at the microwave region. Our results demonstrate that remanence based magnetoplasmons provide a promising way to realize devices below the diffraction limit with new functionalities.

1. Introduction

Surface plasmons, collective oscillations of charge-carriers in conductors or doped semiconductors, provide subwavelength confinement of optical field, and thus hold a great potential in minimizing the scale of optical systems [1–3]. Magnetoplasmons (MPs) are surface plasmons sustained at the interface between a dielectric and a magneto-optical material applied with a static external magnetic field [4–6]. Compared with surface plasmons, MPs can exhibit one-way propagation due to the breaking of the time reversal symmetry by the external magnetic field [7–9]. One-way electromagnetic modes provide a basic mechanism for realizing new classes of photonic devices that would be impossible using conventional reciprocal electromagnetic modes. Based on one-way MPs, the time-bandwidth limit in physics and engineering can be overcome in properly designed waveguide/cavity system [10]. Other potential applications based on one-way MPs, such as high-efficiency tunable Y-branch power splitter [9,11], broadband four-port circulator [12], have also been demonstrated.

Realization of one-way electromagnetic mode generally relies on magneto-optical materials and strong external magnetic field. Recent researches have also shown that two-dimensional (2D) materials can support MPs of topologically protected optical states [13–15]. Though one-way MPs in such magneto-optical materials, from three-dimensional (3D) metals and doped semiconductors to two-dimensional graphene and black phosphorus, exhibit many alluring properties, the requirement of external magnetic field seriously hinders the miniaturization and integration of related optical devices. However, ferrimagnetic materials, as widely used

magneto-optical materials in microwave regime, can preserve gyromagnetic properties after removing the external magnetic field. Hence, based on remanence, it is possible for ferrimagnetic materials to support unidirectional propagating MPs without external magnetic field. Evidently, one-way MP waveguide based on ferrimagnetic remanence is naturally an isolator for optical system at microwave frequencies. As a result of the plasmonic system without external magnetic field, such isolator can be designed as subwavelength scale. In microwave regime, traditional isolators, in which the external magnetic field is applied, generally have narrow band of operation [16], and recently, several configurations of isolators based on MPs have been proposed with use of external magnetic fields [17–19]. On the contrary, isolator based on the remanence and related one-way MP does not need external magnetic field and has the potential to achieve high isolation ratio for a broad band. But one-way MP based on the remanence of ferrimagnetic material and its application in isolator is seldom investigated so far.

In this paper, we theoretically investigate the dispersion properties of MPs in a ferrite-dielectric-ferrite layered structure without any external magnetic field. Both ferrites in the system possess remanences but their magnetization directions are anti-parallel. Two different kinds of guiding mechanism are analyzed as well as the symmetry properties of the guiding modes. Moreover, the coupling between the proposed one-way waveguide and a traditional metal slab waveguide is investigated. We will show that isolator with subwavelength scale can be realized based on remanence. Such isolator can be straightforwardly extended to the 3D case and thus has value of practical application.

2.   Basic physical model

Magneto-optical materials, e.g., metal, doped semiconductor and ferrite, can be characterized by a frequency-dependent permittivity or permeability tensor under a static external magnetic field [20,21]. Noble metals and semiconductors usually lose their gyroelectric properties when the external magnetic field is turned off, and the related permittivity tensor reduces to a scalar. Two-dimensional materials, such as graphene and black phosphorus, also lose their gyroelectric properties after removing the external magnetic field [13–15]. However, ferrimagnetic material with remanence still preserves its gyromagnetic property after removing the external magnetic field, and its permeability has the tensor form:

$$\mu_{\mathbf{m}}(\omega) = \begin{bmatrix} \mu & -i\kappa & 0 \\ i\kappa & \mu & 0 \\ 0 & 0 & 1 \end{bmatrix} \tag{1a}$$

with

$$\mu = 1, \tag{1b}$$

$$\kappa = -\frac{\omega_r}{\omega}, \tag{1c}$$

where ω is the angular frequency, and ω_r is the characteristic circular frequency of the ferrimagnetic material, which is determined by $\omega_r = \mu_0 \gamma M_r$, where μ_0 is the vacuum permeability, γ is the gyromagnetic ratio, and M_r is the remanent magnetization. The off-diagonal terms in Eq. (1) indicate the gyromagnetic feature of the ferrimagnetic material with remanence in the absence of external magnetic field. In this expression for the permeability, the material absorption loss is neglected. The loss of the ferrimagnetic material will be taken into account later when we investigate MPs in realistic systems.

The proposed structure for sustaining one-way MPs is composed of a dielectric slab sandwiched by two ferrimagnetic materials, as illustrated in Fig. 1. The two ferrimagnetic materials with remanent magnetizations in the anti-parallel directions provide a closed magnetic circuit, making

it possible to realize an effective and stable one-way waveguide. The ferrimagnetic materials are assumed to be semi-infinite without loss of generality, because the MPs propagate on the surface of such gyromagnetic materials with electromagnetic fields decay exponentially inside the ferrimagnetic materials. However, for the electromagnetic waves in the dielectric layer, the fields exhibit two kinds of distributions. One refers to the surface mode with the field exponentially decays from the two dielectric-ferrite interfaces. The other refers to the regular mode with the field reflected between the two dielectric-ferrite interfaces. The surface modes (i.e., MPs) are transverse-electric-polarized (TE) in the proposed 2D structure (field along z-axis is assumed to be uniform), and the nonzero component (E_z) of the electric field can be written as

$$E_z(x, y) = Ae^{-\alpha y}e^{ikx}, \qquad y > \frac{d_0}{2} \tag{2a}$$

$$E_z(x, y) = (B_1 e^{-\alpha_d y} + B_2 e^{\alpha_d y})e^{ikx}, \qquad y < \left|\frac{d_0}{2}\right| \tag{2b}$$

$$E_z(x, y) = Ce^{\alpha y}e^{ikx}. \qquad y < -\frac{d_0}{2} \tag{2c}$$

Here k is the propagation constant. $\alpha_d = \sqrt{k^2 - \epsilon_r k_0^2}$ in Eq. (2b) denotes the attenuation coefficient of the field in the dielectric layer, where ϵ_r is the relative permittivity of the dielectric and $k_0 = \omega/c$ is the wavenumber in vacuum; $\alpha = \sqrt{k^2 - \epsilon_m \mu_v k_0^2}$ in Eqs. (2a) and (2c) denotes the attenuation coefficient in the ferrimagnetic materials, where ϵ_m and $\mu_v = (\mu^2 - \kappa^2)/\mu$ are, respectively, the relative permittivity and Voigt permeability of the ferrimagnetic materials. The attenuation coefficients α and α_d in Eq. (2) are both real and positive, denoting that the field decays exponentially away from the two dielectric-ferrite interfaces. The electric field for the regular modes can also be expressed with Eq. (2) by replacing α_d with ik_y, where $k_y = \sqrt{\epsilon_r k_0^2 - k^2}$ is a real and positive number. The nonzero components of the magnetic field (H_x and H_y) can be obtained straightforwardly from Eq. (2), and the boundary conditions require E_z and H_x to be continuous at the dielectric-ferrite interfaces. Based on this, the dispersion relation for the proposed structure is determined and it has the forms

$$\frac{\alpha + \kappa k}{\alpha_d \mu_v} + \tanh \frac{\alpha_d d_0}{2} = 0 \tag{3a}$$

$$\frac{\alpha + \kappa k}{\alpha_d \mu_v} + \coth \frac{\alpha_d d_0}{2} = 0 \tag{3b}$$

for the surface modes, and

$$\frac{\alpha + \kappa k}{k_y \mu_v} - \tan \frac{k_y d_0}{2} = 0 \tag{4a}$$

$$\frac{\alpha + \kappa k}{k_y \mu_v} + \cot \frac{k_y d_0}{2} = 0 \tag{4b}$$

for the regular modes.

It is obvious from Eqs. (3) and (4) that both the surface mode and regular mode can be further classified into two subgroups: one mode with even symmetry and the other with odd symmetry, as a result of the interaction between the two dielectric-ferrite interfaces in the proposed structure. Equations (3a) and (4a) [(3b) and (4b)] describe the dispersion relations of the even(odd) symmetry modes whose electric field component E_z is symmetrical (antisymmetrical) with respect to the x-axis in Fig. 1. When the propagation constant (k) approaches $-\infty$, the fields of the surface modes are highly confined at the dielectric-ferrite interfaces, thus the
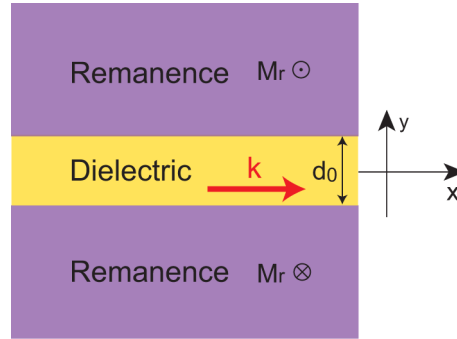
Fig. 1. Schematic of a one-way waveguide based on ferrimagnetic material with remanence. The red arrow indicates the propagating direction and d_0 denotes the thickness of the dielectric layer. The remanent magnetization directions of the gyromagnetic materials are along $\pm \hat{\mathbf{z}}$.

coupling between them becomes negligible. Therefore, when $k \rightarrow -\infty$, the dispersion relations of the surface modes with both symmetries in the proposed structure have the same asymptotic frequency $\omega_{sp} = \omega_r/2$, which is also the asymptotic frequency for MPs propagating along a single dielectric-ferrite interface. Note that ω_{sp} is neither dependent on the mode symmetry nor the thickness of the dielectric layer. On the other hand, the regular modes are highly dependent on the thickness of the dielectric layer. When $\omega < \omega_r$ and for $|k| < \sqrt{\epsilon_r} k_0$ (providing α and k_y to be both real and positive values), the first terms in Eqs. (4a) and (4b) are always negative. Thus, we can find solutions for regular modes with even symmetry when $k_y d_0/2 \in (\pi/2 + n\pi, (n+1)\pi)$, and for regular modes with odd symmetry when $k_y d_0/2 \in (n\pi, \pi/2 + n\pi)$, where $n = 0, 1, 2, \ldots$. Evidently, there is a critical value of d_0, below which only the regular mode with odd symmetry exists in the proposed structure. This critical value is given by

$$d_c = \frac{\lambda_r}{2\sqrt{\epsilon_r}}. \tag{5}$$

3. Modal properties

Figure 2 shows the dispersion relations of MPs propagating in the proposed structure with various dielectric thicknesses. Throughout this paper, we consider yttrium-iron-garnet (YIG) to be the ferrimagnetic material with the characteristic remanent circular frequency $\omega_r = 2\pi \times 3.587 \times 10^9$ rad/s and the relative permittivity $\epsilon_m = 15$ [16]. The dielectric layer is assumed to be air with $\epsilon_r = 1$ when calculating the dispersion relations. As we can see from Fig. 2(a), when the thickness of the dielectric layer is smaller than the critical value d_c, the dispersion curves exhibit different characteristics in different frequency ranges. Firstly, when $\omega < \omega_{sp}$, the surface mode with even symmetry can propagate both forward and backward while the surface mode with odd symmetry is forbidden. Secondly, when $\omega_{sp} < \omega < \omega_r$, see the yellow area in Fig. 2(a), all the three modes, i.e. the surface modes with both symmetries and regular mode with odd symmetry, are unidirectional and immune to backscattering. This specific region is called the complete unidirectional propagating (CUP) region of MPs. At last, when $\omega > \omega_r$, the unidirectional propagating modes suffer from scattering loss because the bulk modes of the ferrimagnetic material with remanence appear in this frequency region. Note that when $k_y d_0/2 \in (0, \pi/2)$, the dispersion curves of the surface mode with odd symmetry and regular mode with odd symmetry are continuous at the light lines, as we can see from Fig. 2. This can be understood from the fact that Eq. (3b) and Eq. (4b) give the same solution when α_d and k_y approach zero, respectively. When the thickness of the dielectric layer d_0 increases [see

from Figs. 2(a) to 2(d)], the modes with even and odd symmetries get closer, approaching the dispersion curve of MPs at a single dielectric-ferrite interface from both sides. In addition, the nth-order regular mode with even symmetry appears when $d_0 > (2n - 1)d_c$, and the nth-order regular mode with odd symmetry appears when $d_0 > 2nd_c$, where $n = 1, 2, 3, \ldots$. It is obvious from Figs. 2(c) and (d) that all the regular modes except the first-order odd symmetry mode can propagate both forward and backward, thus compress the CUP region. Therefore, to preserve a broad CUP band from ω_{sp} to ω_r, the thickness of the dielectric layer needs to be smaller than the critical value d_c. We also numerically analyze the guiding modes in the proposed structure whose dielectric layer is glass with $\epsilon_r = 4.28$ instead of air, and find that the obtained modal dispersion properties are similar to those illustrated in Fig. 2.
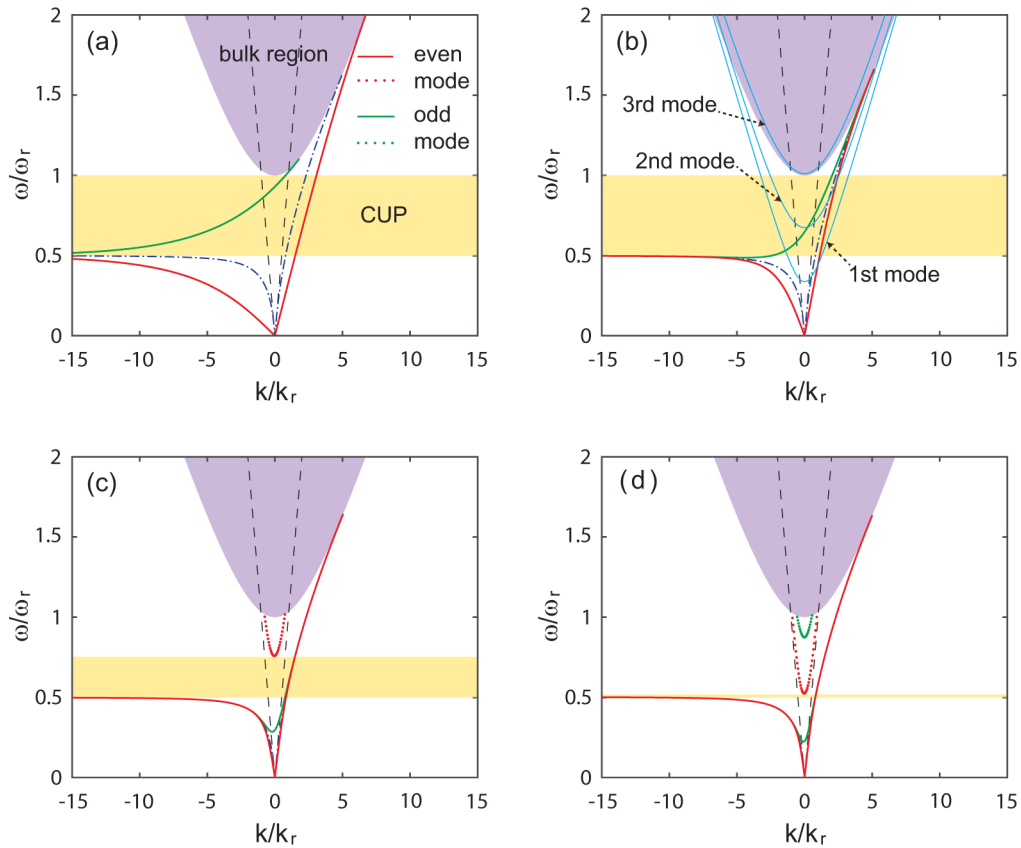
Fig. 2. Dispersion relations of MPs in the proposed structure when the thicknesses of the dielectric layer d_0 are of the values (a) $0.035\lambda_r$, (b) $0.145\lambda_r$, (c) $0.75\lambda_r$ and (d) $1.20\lambda_r$. The red(green) lines represent the dispersion curves of the even(odd) symmetry modes. The dashed lines indicate the light-lines, and the dot-dash lines are the dispersion curves of MPs propagating at a single dielectric-ferrite interface. The purple areas are the zones of bulk modes in the ferrimagnetic materials, and the yellow areas indicate the CUP regions. The light-blue lines in (b) are the first-three order modes of the traditional metal slab waveguide (discussed in Section 4).

In order to investigate the propagation loss in the proposed one-way waveguide, the absorption of the ferrimagnetic material needs to be considered. As a dispersive medium, the ferrimagnetic

material is inherently lossy, and for this case Eqs. (1b) and (1c) become

$$\mu = 1 + \frac{i\nu\omega_r}{\omega^2 + \nu^2}, \tag{6a}$$

$$\kappa = -\frac{\omega\omega_r}{\omega^2 + \nu^2}, \tag{6b}$$

where ν is the relaxation angular frequency. The energy loss of MP can be characterized by its propagation length determined by $L = 1/(2k_i)$, where k_i is the imaginary part of the propagation constant. In the case of $\nu \ll \omega_r$, the loss of the MP is proportional to the fraction of electromagnetic energy in the ferrimagnetic material. Correspondingly, the larger the electromagnetic energy fraction of MP is distributed within the dielectric layer, the larger the propagation length is. Therefore, the mode with even symmetry tends to propagate longer than that with odd symmetry, because the electromagnetic field vanishes at $y = 0$ in the dielectric layer for the odd symmetry mode. To verify the analysis above, we calculate the propagation constants for various dielectric thicknesses d_0, and the results are plotted in Fig. 3. The operating frequency is set to be $\omega = 0.75\omega_r$, which just lies at the center of the CUP region. The relaxation angular frequency is $\nu = 5 \times 10^{-3}\omega$, and other parameters are the same as in Fig. 2. Two dielectric cases of air and glass are considered. As shown in Fig. 3(a), where the dielectric layer in the waveguide is air, the propagation length of the mode with odd symmetry increases with the air thickness and finally approaches to $L_s = 13.51\lambda_r$, which corresponds to the propagation length of MP propagating at a single ferrite-air interface. For the mode with even symmetry, the propagation length first increases with d_0 because more electromagnetic energy fraction is distributed in the dielectric layer. The propagation length L reaches its maximum of $15.7\lambda_r$ when $d_0 = 0.2\lambda_r$, afterwards, the coupling between the two ferrite-air interfaces become weaker thus L approaches to L_s as d_0 continuously increasing. Figure 3(b) presents similar results when the dielectric layer in the proposed structure is glass instead of air. But the propagation length for the present case is larger than that for the former case [shown in Fig. 3(a)]. The maximal propagation length for the glass case is found to be $25.68\lambda_r$, which occurs at $d_0 = 0.46\lambda_r$. This phenomenon can be understood from the fact that a dielectric layer with higher permittivity in the proposed structure provides a larger capacity for modal electromagnetic energy.
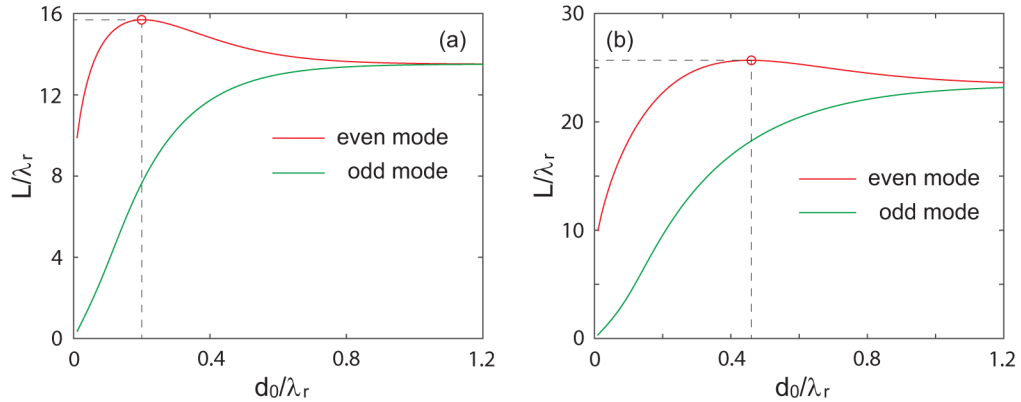
**Fig. 3.** Propagation lengths for MPs as a function of the dielectric thickness d_0 when $\omega = 0.75\omega_r$. The dielectrics are assumed to be air with $\epsilon_r = 1$ in (a) and glass with $\epsilon_r = 4.28$ in (b). The red lines indicate the modes with even symmetry and the green lines are odd symmetry modes. The maximal propagation length for the mode with even symmetry is marked with a red circle in each panel.

4.   Subwavelength isolator

After clarifying the dispersion and loss properties of MPs in the proposed one-way waveguide, we now consider its application in an optical system as a broadband isolator with subwavelength scale. The coupling between a plasmonic waveguide and a traditional optical waveguide is challenging due to the different modal field profiles in the two systems. However, in the proposed one-way waveguide, the electric field distribution of the surface mode with even symmetry is similar to that of the fundamental TE mode in a traditional metal slab waveguide when the dielectric thickness d_0 is relatively small. Thus it is possible to realize an efficient coupling between these two systems with proper design. To clarify this, we first perform the numerical simulation of wave transmission in the system of a metal slab waveguide linked to the proposed one-way waveguide, with the finite element method (FEM) using commercial (COMSOL Multiphysics) software. In the simulation, the metal is assumed to be perfectly electric conductor, which is a good approximation in the microwave regime. To make the modal sizes in the two coupled waveguides be comparable, the metal slab waveguide is filled with silicon of $\epsilon_d = 11.9$. The distance between the two metal slabs d_p [as depicted in Fig. 5(c)] satisfies $\lambda_r/\sqrt{\epsilon_d} < d_p < 3\lambda_r/(2\sqrt{\epsilon_d})$, ensuring that the third-order TE mode with even symmetry lies outside the CUP region [see the light-blue lines in Fig. 2(b)]. Thus, there exists only one mode with even symmetry (in the metal slab waveguide) in the CUP range. In the simulation, we use an input port with a fundamental TE mode to excite wave at the open end of the metal slab waveguide. Note that the second-order TE mode of the metal slab waveguide cannot be excited because its symmetry is different from that of incident field. Figure 4 shows the coupling performance of the metal slab waveguide (with the fundamental TE mode) to the proposed one-way waveguide. The length of the one-way waveguide is $L_0 = \lambda_r$ and the relaxation angular frequency is $\nu = 5 \times 10^{-3}\omega$. It is evident that the reflection at the interface between the two waveguides is very sensitive to d_0 and d_p, and we obtain the optimal coupling when $d_0 = 0.145\lambda_r$ and $d_p = 0.43\lambda_r$, at which the transmission efficiency reaches the maximum of 95.14%, while the reflectance is only 0.72%. Note that the single-mode transmission in the metal slab waveguide requires that $d_p \leq 0.43\lambda_r$.
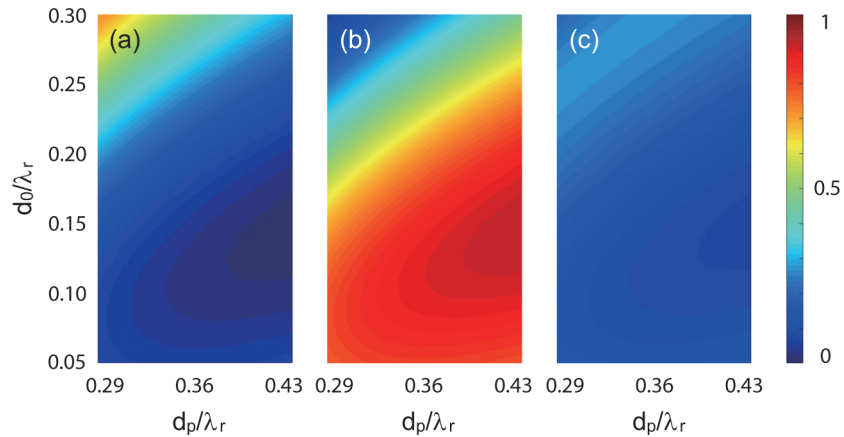
Fig. 4. Reflection (a), transmission (b) and absorption (c) as a function of the dielectric thickness d_0 and the distance of the two metal slabs d_p when the fundamental TE mode of a metal slab waveguide is coupled into the proposed one-way waveguide. The operating frequency is $0.75\omega_r$ and the relaxation angular frequency of YIG is $\nu = 5 \times 10^{-3}\omega$. The dielectric filled in the metal slab waveguide is silicon with $\epsilon_d = 11.9$.

Based on the results obtained above, we propose an isolator consisting of the one-way waveguide and two metal slab waveguides, as shown in Figs. 5(b) and 5(c). The wave transmission in
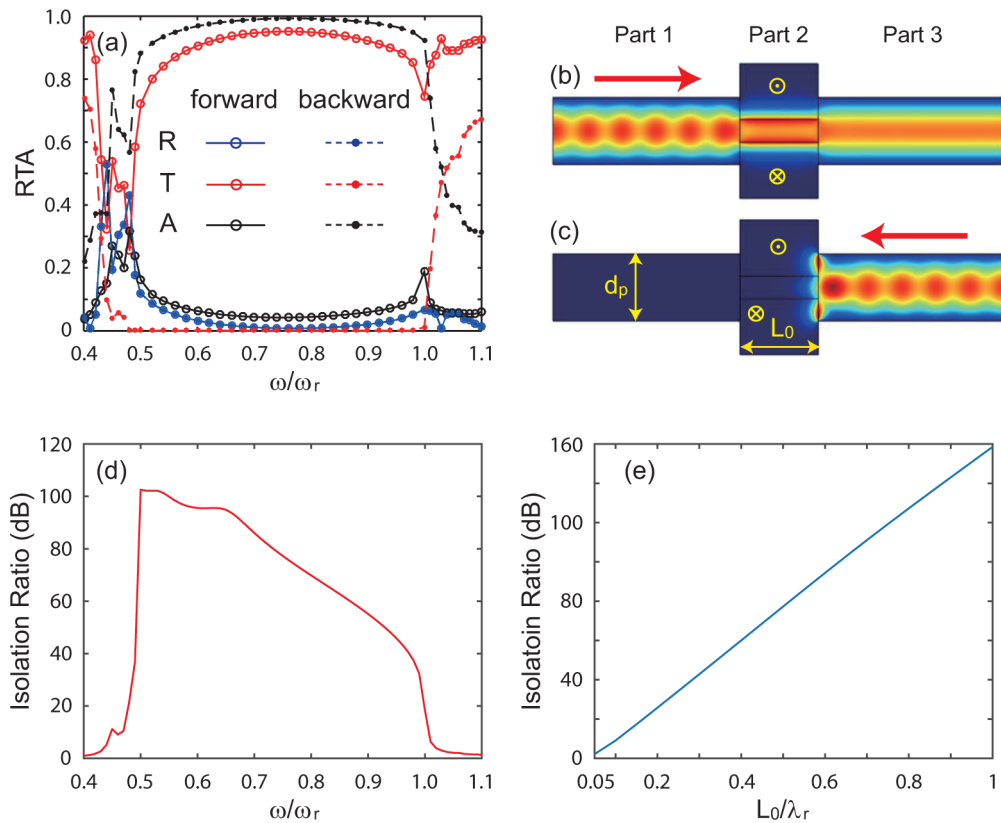
Fig. 5. (a) Reflection, transmission and absorption as a function of frequency for both forward and backward propagating directions of the isolator. Solid lines with circles denote the forward propagation while dashed lines with dots for the backward propagation. The dielectric thickness of the one-way waveguide is $d_0 = 0.145\lambda_r$, the distance between the two metal slabs is $d_p = 0.43\lambda_r$, and the length of the one-way waveguide is $L_0 = 0.5\lambda_r$. (b)-(c) Electric field distributions for the forward and backward directions when the operating frequency $\omega = 0.75\omega_r$, respectively. Red arrows denote the propagating directions of the electromagnetic wave. (d) The isolation ratio as a function of frequency when $L_0 = 0.5\lambda_r$ and $\omega = 0.75\omega_r$. (e) The isolation ratio as a function of the length of the one-way waveguide when $\omega = 0.75\omega_r$.

this isolator system is simulated with the FEM. Figure 5(b) shows the simulated electric field amplitudes for the case when the input port is placed at the left end of isolator system. For a forward propagating wave with frequency in the CUP region, the fundamental TE mode in Part 1 converts to the plasmonic mode with even symmetry in Part 2, the reflection here is minimized as discussed above. Afterwards, the plasmonic mode propagates through Part 2 and converts back to the fundamental TE mode without any backscattering in Part 3, as illustrated in Fig. 5(b). On the contrary, when we reverse the propagating direction, the electromagnetic wave is blocked by Part 2, as illustrated in Fig. 5(c). Figure 5(a) shows the simulated values of wave transmission, reflection, and absorption in the isolator as a function of frequency. For both the forward and backward propagating directions, there are two influence factors for the wave transmission. One is the reflection when the input electromagnetic wave first reaches Part 2, and other is the absorption by the ferrimagnetic materials. The reflection is the same for both propagating directions in the whole frequency spectrum, while the absorption increases dramatically for the backward

propagating wave in the CUP region. In the broad frequency range from $0.6\omega_r$ to $0.93\omega_r$ (within the CUP region), the transmission of the forward propagating wave is above 90%, while that of the backward propagating wave is below 0.00093%. When the operating frequency is below the CUP region, Part 2 is no longer unidirectional, it works as a cavity and the isolation ratio is greatly reduced. If the isolator works at a frequency above the CUP region, the transmission for both propagating directions increases because the electromagnetic wave can propagate inside the ferrimagnetic materials. Thus the isolation ratio also decreases at this frequency region. Therefore, only within the CUP region, the proposed system provides sufficient isolation ratio, for example, from $0.6\omega_r$ to $0.93\omega_r$, the isolation ratio is above 49dB, as shown in Fig. 5(d). In order to realize a compact optical isolator, we further calculate the isolation ratio as a function of the length (L_0) of the unidirectional propagating part, and the obtained results are plotted in Fig. 5(e). The field strength of backward propagating wave decays exponentially along the backward direction within Part 2, as a result, the isolation ratio (in dB) is almost linearly related to L_0. It is found that the proposed isolator can provide 42dB isolation ratio when its length is only $0.3\lambda_r$.

Finally, we point out that our proposed 2D isolator can be straightforwardly extended to the 3D case. To show this, a 3D isolator system is constructed by terminating the 2D system in the z direction with two metal slabs, i.e., the isolator has a finite width in the lateral direction. The simulated results for wave transmission in this 3D system are plotted in Fig. 6. Obviously, the field distributions are exactly the same as those in Figs. 5(b) and 5(c) on the xy plane, while they are still uniform along the z axis. This can be understood from the fact that the electric fields of the modes supported in the proposed isolator is along the z direction, which naturally satisfies the boundary conditions in the lateral direction. So the fields in the 3D system is physically identical to those in the 2D system. Therefore, our results previously obtained for the 2D cases are meaningful in practice. Clearly, broadband subwavelength isolator at microwave frequencies can be realized based on the remanence of ferrimagnetic material.
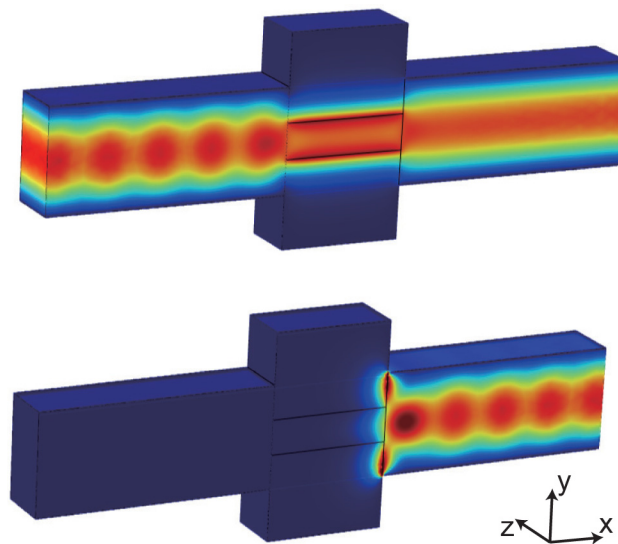
Fig. 6. Three dimensional simulation results of the isolator extended from our 2D case. The width in the z-axis is 20mm and other parameters are the same as in Figs. 5(b) and 5(c).

5. Conclusions

We have demonstrated that broadband unidirectional propagation of MPs at microwave frequencies can be realized by use of the ferrimagnetic material with remanence. In the related waveguide system, which consists of a dielectric slab sandwiched by two ferrimagnetic materials with anti-parallel remanent magnetizations, no external magnetic field is required. The dispersion relations for MPs in this system have been systematically investigated, and the effects of the dielectric thickness on the dispersion and propagation length of MPs are also carefully addressed. Our results show that the proposed structure can provide a robust one-way region for the surface modes with both symmetries and the regular mode with odd symmetry. Compared with the odd-symmetry mode, the even-symmetry mode possesses a longer propagation length because its electromagnetic energy is more distributed within the dielectric layer. Additionally, due to the similar modal profiles of the surface mode with even symmetry in the proposed structure and the fundamental TE mode in a metal slab waveguide, efficient coupling between these two waveguides can be achieved with the proper design. Relying on our studied one-way waveguide, we have proposed a high-quality subwavelength isolator with no external magnetic field applied. The good performance of such an isolator has been verified by numerical simulation. All results obtained in the 2D cases can be straightforwardly extended to the corresponding 3D systems, therefore they are meaningful in practice. The proposed one-way MPs based on remanence have promising applications in constructing new compact optical components with extremely high quality, e.g., broadband ioslator with subwavelength size, field enhancement devices for sensing or enhanced nonlinearity.

Funding

References

1. E. Ozbay, "Plasmonics: Merging photonics and electronics at nanoscale dimensions," Science **311**(5758), 189–193 (2006).
2. S. A. Maier, *Plasmonics* (Springer-Verlag GmbH, 2007).
3. D. K. Gramotnev and S. I. Bozhevolnyi, "Plasmonics beyond the diffraction limit," Nat. Photonics **4**(2), 83–91 (2010).
4. Z. Yu, G. Veronis, Z. Wang, and S. Fan, "One-way electromagnetic waveguide formed at the interface between a plasmonic metal under a static magnetic field and a photonic crystal," Phys. Rev. Lett. **100**(2), 023902 (2008).
5. V. Kuzmiak, S. Eyderman, and M. Vanwolleghem, "Controlling surface plasmon polaritons by a static and/or time-dependent external magnetic field," Phys. Rev. B **86**(4), 045403 (2012).
6. L. Shen, Y. You, Z. Wang, and X. Deng, "Backscattering-immune one-way surface magnetoplasmons at terahertz frequencies," Opt. Express **23**(2), 950 (2015).
7. H. Zhu and C. Jiang, "Broadband unidirectional electromagnetic mode at interface of anti-parallel magnetized media," Opt. Express **18**(7), 6914 (2010).
8. B. Hu, Q. J. Wang, and Y. Zhang, "Broadly tunable one-way terahertz plasmonic waveguide based on nonreciprocal surface magneto plasmons," Opt. Lett. **37**(11), 1895 (2012).
9. X. Zhang, W. Li, and X. Jiang, "Confined one-way mode at magnetic domain wall for broadband high-efficiency one-way waveguide, splitter and bender," Appl. Phys. Lett. **100**(4), 041108 (2012).
10. K. L. Tsakmakidis, L. Shen, S. A. Schulz, X. Zheng, J. Upham, X. Deng, H. Altug, A. F. Vakakis, and R. W. Boyd, "Breaking lorentz reciprocity to overcome the time-bandwidth limit in physics and engineering," Science **356**(6344), 1260–1264 (2017).
11. J. Zou, Y. You, X. Deng, L. Shen, J.-J. Wu, and T.-J. Yang, "High-efficiency tunable y-branch power splitters at terahertz frequencies," Opt. Commun. **387**, 153–156 (2017).
12. K. Liu, A. Torki, and S. He, "One-way surface magnetoplasmon cavity and its application for nonreciprocal devices," Opt. Lett. **41**(4), 800 (2016).
13. P. A. D. Gonçalves and N. M. R. Peres, *An Introduction to Graphene Plasmonics* (WORLD SCIENTIFIC, 2015).
14. D. Pan, R. Yu, H. Xu, and F. J. G. de Abajo, "Topologically protected dirac plasmons in a graphene superlattice," Nat. Commun. **8**(1), 1243 (2017).
15. Y. You, P. A. D. Gonçalves, L. Shen, M. Wubs, X. Deng, and S. Xiao, "Magnetoplasmons in monolayer black phosphorus structures," Opt. Lett. **44**(3), 554 (2019).

16. D. M. Pozar, *Microwave Engineering* (John Wiley and Sons Ltd, 2011).
17. C. K. Seewald and J. R. Bray, "Ferrite-filled antisymmetrically biased rectangular waveguide isolator using magnetostatic surface wave modes," IEEE Trans. Microwave Theory Tech. **58**(6), 1493–1501 (2010).
18. M. F. Farooqui, A. Nafe, and A. Shamim, "Inkjet printed ferrite-filled rectangular waveguide x-band isolator," in *2014 IEEE MTT-S International Microwave Symposium (IMS2014)*, (IEEE, 2014).
19. W. Marynowski, "Integrated broadband edge-guided mode isolator with antiparallel biasing of the ferrite slabs," IEEE Microw. Wirel. Components Lett. **28**(5), 392–394 (2018).
20. J. J. Brion, R. F. Wallis, A. Hartstein, and E. Burstein, "Theory of surface magnetoplasmons in semiconductors," Phys. Rev. Lett. **28**(22), 1455–1458 (1972).
21. A. Hartstein, E. Burstein, A. A. Maradudin, R. Brewer, and R. F. Wallis, "Surface polaritons on semi-infinite gyromagnetic media," J. Phys. C: Solid State Phys. **6**(7), 1266–1276 (1973).